TOWARDS ADDITIVE MANUFACTURING OF RAMIFIED SCAFFOLDS OF THE THYROID VASCULAR SYSTEM: A PRELIMINARY FRACTAL ANALYSIS

E. Bassoli, L. Denti and A. Gatto

Univ. of Modena & Reggio Emilia, Dept. of Engineering "Enzo Ferrari" (DIEF), Modena, Italy

G. Spaletta

Dept. of Mathematics, Univ. of Bologna, Bologna, Italy

M. Sofroniou

Wolfram Research, Champaign-Urbana, Illinois, U.S.A

A. Parrilli, M. Fini and R. Giardino

Preclinical and Surgical Studies Lab.- RIT- BITTA Lab., Rizzoli Orthopaedic Institute, Bologna, Italy

A. Zamparelli

Lab. of Musculoskeletal Cell Biology, IOR-Bologna, Italy

N. Zini

Institute of Molecular Genetics-Section of Bologna, National Research Council, IOR-Bologna, Italy

F. Barbaro, E. Bassi, S. Mosca and D. Dallatana

Dept. and Museum of Biomedical, Biotechnological, and Translational Sciences (S.Bi.Bi.T.) - Lab. of Regenerative Morphology and Bioartificial Structures, Univ. of Parma School of Medicine (Italy)

R. Toni

Dept. and Museum of Biomedical, Biotechnological, and Translational Sciences (S.Bi.Bi.T.) - Lab. of Regenerative Morphology and Bioartificial Structures, Univ. of Parma School of Medicine (Italy) and Division of Endocrinology, Diabetes and Metabolism, Tufts Medical Center - Tufts University School of Medicine, Boston, MA (USA)

Towards Additive Manufacturing of ramified scaffolds of the thyroid vascular system: a preliminary fractal analysis

ABSTRACT

Fractal properties have been demonstrated in literature for several human vascular systems. In the frame of the investigation of additive manufacturing (AM) as a viable solution to prototype single arterial branches of human soft tissue organs, the paper provides a fractal analysis of the arterial tree of the human thyroid gland. The possibility that the thyroid arterial structure may be described as auto-similar is investigated, by studying injection-corrosion casts of the cadaveric gland. Vessel branching is analyzed by measuring branch diameters, ramification angles, and vessel lengths with the use of an optical microscope. Metrological results are made dimensionless by applying, as a scaling parameter, the caliber of major arteries. Data are then studied on a cumulative basis and processed to infer general rules for vessel branching. High resolution microtomography (mCT) is used to determine the spaces occupied by vascular branches and calculate their planar fractal dimension. Finally, the vascular tree has been simulated by a mixed, stochastic / deterministic algorithm based on diffusion limited aggregation (DLA), in which mean values of vascular variables are set as constraints. The purpose of this research is to understand if fractality can be reliably assumed for computational modeling of the organ anatomy, in order to be able to produce, by AM, more representative physical prototypes and scaffolds. The finding allow to affirm that the human thyroid arterial structure exhibits a degree of auto-similarity

1. INTRODUCTION

Recently, we developed a combined additive layer manufacturing / indirect replication method to prototype single arterial branches of human soft tissue organs, including the thyroid gland (Bassoli et al., 2011, 2012). There is increasing evidence that the three-dimensional (3D) geometry of native stromal-vascular scaffolds (SVS) and biomaterial-based scaffolds are key regulators of cell growth and differentiation in *in vivo* and in *ex situ* (i.e. on the laboratory bench) engineered, bioartificial organs (Toni et al., 2008, 2011). Thus, we have investigated geometrical properties of the intraglandular vascular component of the natural SVS of the adult, human thyroid (Parrilli et al., 2013). In particular, we have focused on the possible fractal organization of its arterial network, based on the report that a number of human arterial systems have fractal geometry (Zamir, 2001). Presence of auto-similarity in the anatomy of the thyroid SVS would imply that 3D cell growth during natural development and *ex situ* regenerations of the thyroid tissue occurs in a space phase with trajectories dictated by its fractal structure. As a result, *ex situ* reconstruction of the entire organ might take place through cellular self-assembly guided by the rules of the chaotic attractor inherent to the SVS geometry (Toni et al, 2007). Finally, since auto-similarity is consistent at different size scales, knowledge of any random part of the SVS, e.g. obtained by imaging techniques on *in vivo* subjects, might allow for computational modeling and eventual AM with biomaterials of patient's tailored SVS mimicking the 3D morphology of the native thyroid gland (Toni et al., 2007, 2011). Therefore, we conducted a study on vascular fractality using three different

E. Bassoli, L. Denti, A. Gatto, G. Spaletta, M. Sofroniou, A. Parrilli, M. Fini, R. Giardino, A. Zamparelli, N. Zini, F. Barbaro, E. Bassi, S. Mosca, D. Dallatana and R. Toni

approaches, including 3D vascular casts of the cadaveric thyroid, branches of the intraglandular thyroid arteries prototyped by AM, and a computational 3D reconstruction of the arterial component of the adult thyroid SVS.

2. MATERIALS AND METHODS

The overall experimental design is outlined in Figure 1, and described below.

2.1. Preparation of 3D thyroid vascular casts

3D casts of the intraglandular arterial network of the adult human thyroid were prepared from glands obtained at autopsy, using a well-established technique (Toni et al. 2007, 2011). Shortly, superior and inferior thyroid arteries were injected with a solution of 3% polyvinyl chloride-co-vinyl acetate (Pevikon C 870, Sigma- Aldrich) diluted in acetone, to fill the intraglandular vascular fields. After resin polymerization, the thyroid tissue was digested by immersion in a solution of 5% HCL / pepsin for 48-72 hours, leading to retrieval of the glandular arterial network.

2.2. Morphometry of 3D thyroid vascular casts

Ramification features of the intra-lobar thyroid arteries were preliminarily measured on a single thyroid cast as outlined in the following:

- The vascular cast was arbitrarily divided into 7 measuring fields, on the basis of simple symmetries of vascular architecture, as shown in Figure 2. Using a WILD N3Z Heerbrugg stereomicroscope, images of all fields were collected at different focal distances, and digitally acquired.

- Then, five vascular areas were randomly selected, and measured using a Kestrel 200 measuring microscope, equipped with Quadra-check metrology software (Vision Engineering). These high accuracy readings were used to set metrical references in terms of pixels, to be eventually attributed to any other digital image of the cast subjected to analysis (calibration procedure).
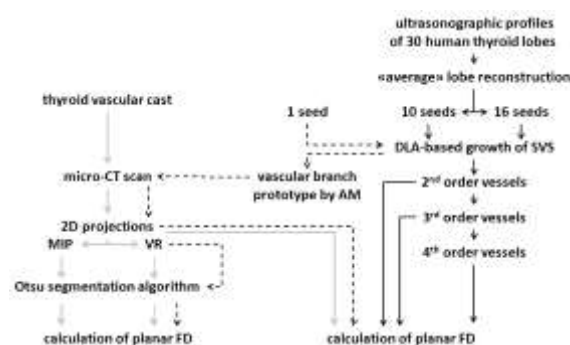
Figure 1 Outline of the experimental procedure. Values of fractal dimension (FD) were obtained using: 1) a vascular computational modeling (solid dark lines); b) a prototyped vascular branch (dashed lines); c) an anatomical vascular cast (solid light lines). For details see Materials and MethodsFinally, vessel diameters, ramification angles, and branch lengths were measured on all digitally acquired images of the cast, as depicted in Figure 3 (Schreiner & Buxbaum, 1993; Zamir, 1982). This procedure was repeated at dorsal and ventral sides of the cast.

All measurements were taken assuming: a) single branching, as an isolated vessel branching off from the main one (usually at 90°) without further ramifications; b) multiple branching, as a secondary branch forking off the main one, and leading to further

ramifications; c) bifurcation, if a vessel split into two similar branches, none of which recognizable as the main one.

Table 1 summarizes the different vascular variables measured, whereas Table 2 depicts the ranges of thyroid arterial calibers (i.e. internal diameters) as reported in the anatomical literature (Major, 1909; Papadatos, 1981). To reduce the bias of vascular distortion due to the pressure of intravascular resin injection, diameter size was made dimensionless through the use of a scaling parameter set on the diameter of the superior thyroid artery.

Figure 2 Ventral view of the thyroid cast segmented by measuring fields.
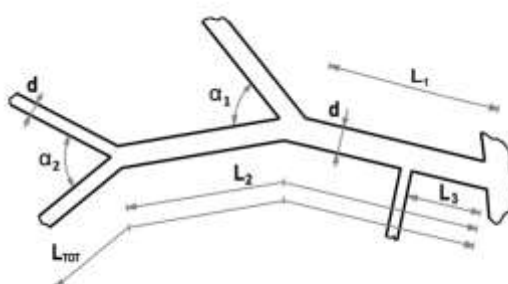
Figure 3 Schematic outline of the analyzed vascular variables.

Table 1 List of morphometrical measurements.

Total length	LTOT
Length before complex branching	L1
Length before bifurcation	L2
Length before single branching	L3
Complex branching angle	α1
Bifurcation angle	α2
Branch diameter	Φ

Table 2 Caliber range (mm) referred to each order of adult, human thyroid arteries (Major, 1909; Papadatos, 1981).

First order	>0.43
Second order	0.09 - 0.43
Third order	0.03 - 0.09
Fourth order	<0.03

E. Bassoli, L. Denti, A. Gatto, G. Spaletta, M. Sofroniou, A. Parrilli, M. Fini, R. Giardino, A. Zamparelli, N. Zini, F. Barbaro, E. Bassi, S. Mosca, D. Dallatana and R. Toni

2.3. Planar (2D) fractal analysis of 3D thyroid vascular casts, and arterial branches obtained by AM

An analysis of the 2D fractal dimension (FD) of the same vascular cast analyzed at 2.2 was performed as summarized in the following.

- A single lobe of the cast was scanned with the microtomographic system Skyscan 1172 (Bruker mCT, Belgium) at the nominal resolution of 30 µm. The sample was rotated up to 180° with a rotation step of 0.4°, and a frame averaging of 4. Source voltage was set at 60 kV while the source current was 167 µA. The reconstruction was performed using a NRecon software (version 1.6.2.0, Bruker mCT, Belgium), and corrections applied where needed, except for the specific misalignment in each acquisition, and a medium ring artifact reduction.

- In a similar manner, a single branch of the intraglandular arterial network of the adult human thyroid obtained by computer modeling with single source seed (see section 2.4), and layer manufactured with acrylic resin through multijet deposition (Bassoli et al., 2011, 2012), was scanned using mCT (source voltage 20kV, current 120 µA), as described above.

- Then, each reconstructed image dataset was used to give rise to 2D images of interest, either lobe or single branch, in three orthogonal planes with Maximum Intensity projection (MIP) and Volume Rendering (VR) techniques. Both techniques allowed for representation of the 3D volumes on a single plane, keeping unaltered the original metrical proportions (Fishman et al., 2006; Pavone et al., 2001).

- Finally, each of the 2D images was automatically segmented (Liao et al., 2001; Pal & Pal, 1993), and threshold for segmentation set using the method proposed by Otsu in a 2-level mode (Otsu, 1979). FD was computed by the box counting method.

2.4. Planar (2D) fractal analysis of 3D numerical - computational simulations of the intraglandular arterial network of the adult human thyroid

An hybrid, fractal / deterministic modeling (DLA algorithm) of the 3D arterial network of the adult human thyroid growing inside a reconstructed thyroid lobe (Spaletta, 2004) was obtained based on deposition of "seeds" along specific sites of the lobe profile (Toni et al., 2007, 2011; Bassoli et al., 2011). In this series of experiments, we decided to reconstruct the arterial network inside an averaged lobe simulation resulting from a group of 30 lobar profiles collected *in vivo* by ultrasonography. Mean number of intraglandular arterial branches, mean arterial calibers from the 2nd to 4th vessel order (see Table 2), and the Murray's law were selected as vascular variables for seed growth. Two different simulations of the thyroid arterial network were computed, using 10 and 16 source seeds, respectively. Each of the two lobar simulations was representative of the intraglandular growth of thyroid arteries up to the 4th vessel order. Then, an analysis of the 2D FD of the computer simulations was performed as follows:

- Each image of the dynamic, 3D arterial network reconstruction was saved as a static 2D image, and projected on a plane arbitrarily chosen.

- The 2D image was saved in standard jpeg format, and the box counting method applied, through implementation (here referred to as MA) in the Mathematica software environment (Wolfram, 2002, Smith et al, 1996). Robustness of this procedure for computing FD was also tested on 2D images obtained as described at 2.3, including the vascular cast, and the single branch prototype.

3. RESULTS

3.1. Morphometry of a 3D thyroid vascular cast

Figure 4 shows an example of the digital images used for cast analysis, whereas results of morphometrical measurements are listed in Table 3. Since pressure of resin injection was expected to modify the original size of the vascular branches, all diameter measurements were made dimensionless, and expressed in terms of percentages with respect to the diameter of the major vessel available, i.e. the superior thyroid artery (2.45 mm). In contrast, metrical values were maintained for branch lengths. The number of measured 4th order vessels was considerably smaller than that of higher order arteries, and these vessels did not show single branchings or bifurcations, possibly due to morphometric underestimation as a consequence of poor penetration of the resin at the finest levels. In all vessel orders measured, diameters and branch lengths decreased proportionally, as opposed to branching and bifurcation angles that remained unchanged. Finally, a comparison between mean diameters from the 1st to the 3rd vascular order depicted a similar scale factor (0.3) that, however, was lost at the finest vessel level (4th order).
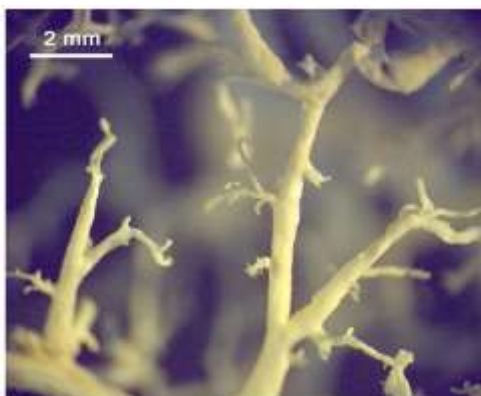
**Figure 4** Optical microscope image used for morphometrical analysis.

Table 3 Morphometric measurements: mean value, standard deviation (SD) and number of observations (N)

	1st order vessels			2nd order vessels		
	mean	SD	N	mean	SD	N
L_{TOT} (mm)	8.26	2.166	79	3.18	1.092	144
L_1(mm)	2.94	1.228	68	1.42	0.628	104
L_2(mm)	4.94	1.803	70	2.16	0.881	106
L_3(mm)	3.06	1.366	29	1.56	0.710	37
α_1(°)	57.7	11.40	50	60.0	11.55	81
α_2(°)	58.6	11.14	43	58.4	14.12	76
Φ (%)	31.5	10.10	209	9.0	3.31	370
	3rd order vessels			4th order vessels		
	mean	SD	N	mean	SD	N
L_{TOT} (mm)	0.55	0.203	126	0.21	0.107	27
L_1(mm)	0.24	0.078	67	0.18	0.040	9
L_2(mm)	0.37	0.142	47	-	-	-
L_3(mm)	0.29	0.104	21	-	-	-
α_1(°)	53.8	10.45	65	47.7	12.83	9
α_2(°)	54.1	10.85	49	-	-	-
Φ (%)	2.4	0.59	235	1.1	0.06	35

E. Bassoli, L. Denti, A. Gatto, G. Spaletta, M. Sofroniou, A. Parrilli, M. Fini, R. Giardino, A. Zamparelli, N. Zini, F. Barbaro, E. Bassi, S. Mosca, D. Dallatana and R. Toni

3.2. Planar (2D) fractal analysis of a 3D thyroid vascular cast, and single arterial branch obtained by AM

Figure 5 shows the XY projections of the mCT scan of the thyroid lobe cast, as obtained using the MIP and VR techniques. Following segmentation with the Otsu algorithm (images on the right column), 2D FD was calculated, and values reported in Table 4. The procedure was applied for each of the three reference planes. The two projection procedures led to differences in the FD values of no more than 4%, while the maximum deviation of FD on different orientations was 7%, proving good robustness against the effects of projection. A similar value of deviation was also observed when comparing FD values computed via MA with respect to mCT procedures.
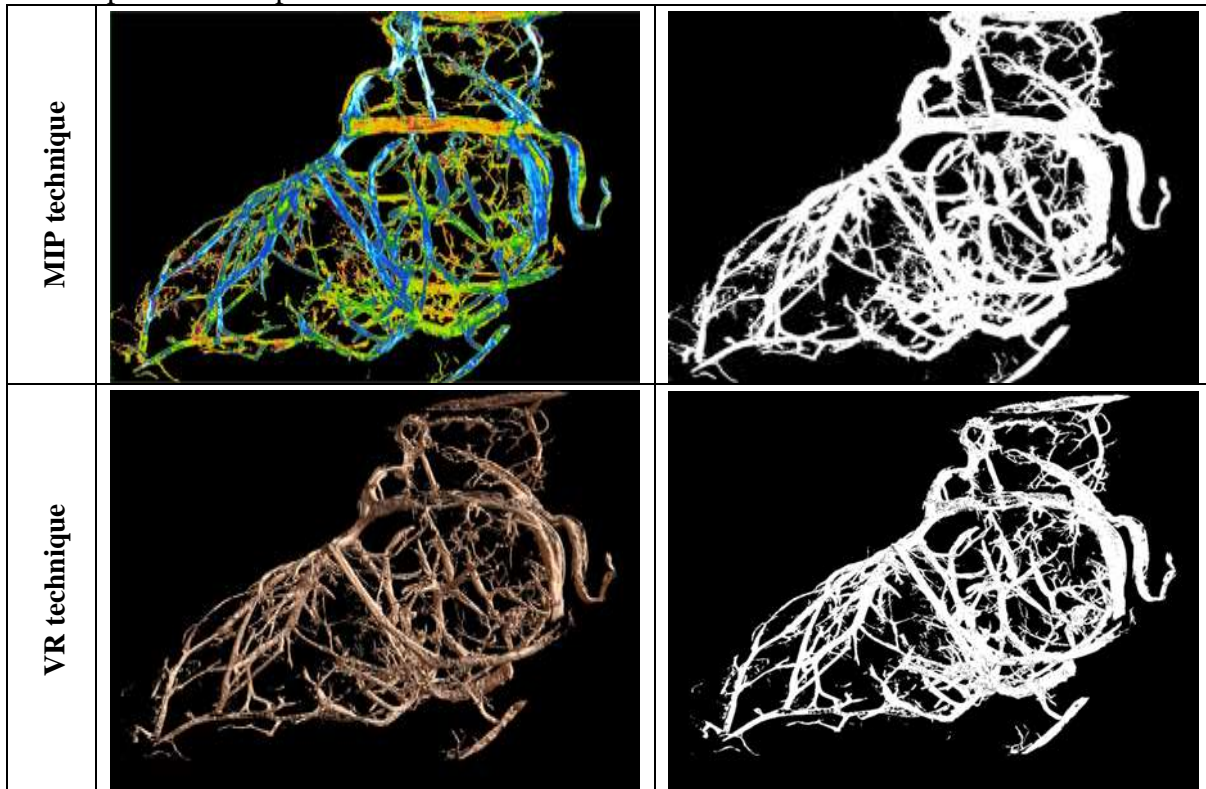
Figure 5 Images of the thyroid vascular cast obtained by mCT: XY projection using the MIP and VR techniques, followed by segmentation through the Otsu algorithm

Differently, 2D FD values taken on the branch prototype diverged from 10% to 20%, depending on the calculation technique used, as depicted in Table 5. Finally, differences in FD values between the cast and resin prototype accounted for 4% - 12%, depending on the VR or MIP techniques, respectively.

Table 4 2D FD of the arterial cast, as obtained by the box counting either through mCT techniques, or Mathematica algorithm (MA)

	MIP technique		VR technique	
	mCT	DLA	mCT	DLA
XY projection	1.817	1.793	1.740	1.800
XZ projection	1.870	1.743	1.835	1.660
YZ projection	1.873	1.811	1.857	1.724

Table 5 2D FD of the single branch prototype, as obtained by the box counting, either through mCT techniques, or Mathematica algorithm (MA)

	MIP technique		VR technique	
	mCT	DLA	mCT	DLA
XY projection	1.612	1.960	1.780	1.763
XZ projection	1.695	1.592	1.800	1.639
YZ projection	1.657	1.597	1.810	1.660

3.3. Planar (2D) fractal analysis of a 3D numerical - computational simulation of the intraglandular arterial network of the adult human thyroid

Values for 2D FD in each of the averaged simulations of the thyroid arterial network are listed in Table 6. FD was poorly affected by the number of source seeds, i.e. by the number of starting vascular branches. However, the network model obtained using only 2nd order branches resulted far less complex than those ensuing from 3rd and 4th order vessels, the latter showing minimal FD differences between them.

Table 6 2D FD of the DLA models in relation to the number of source seeds, and branch order

order of branches	10 seeds	16 seeds
2nd	1.473	1.504
2nd and 3rd	1.651	1.652
2nd, 3rd and 4th	1.657	1.658

4. DISCUSSION

In this report we have shown that the intraglandular arterial network of the adult human thyroid has a fractal nature, as reported for a number of other human vascular systems (Zamir, 2001). The FD was calculated based on the classical box counting method, and values computed as planar dimensions (2D), on the assumption that orthogonal projections of fractals onto a lower-dimensional subspace retain the original non-integer features (Mandelbrot, 1982). In addition, although we used different procedures to project the 3D vascular geometry onto a 2D level, the FD values depicted reciprocal consistency. This result was supported by the observation that an identical scale factor was measured between at least three of the four vessel orders constituting the real intraglandular network. Finally, computer simulation revealed that a specific intraglandular vessel type (primarily the 3rd order branch) was sufficient to describe the occupation of space, and spatial complexity of the entire gland. Resolution limits intrinsic to the imaging techniques used suggest that further studies are needed to optimize data at the level of the finest arterial branches. All these data indicate that the technological chain necessary for production with AM of prototypes of the 3D vascular network in the adult human thyroid is based on a robust information coherent with the starting mathematical model. Consequently, we predict that patient's tailored, 3D ramified scaffolds could be manufactured using random measurements of few morphometric parameters of the native, intraglandular vascular morphology.

ACKNOWLEDGEMENTS

E. Bassoli, L. Denti, A. Gatto, G. Spaletta, M. Sofroniou, A. Parrilli, M. Fini, R. Giardino, A. Zamparelli, N. Zini, F. Barbaro, E. Bassi, S. Mosca, D. Dallatana and R. Toni

REFERENCES

[1] Bassoli, E., Denti, L., Gatto, A., Paderno, A., Spaletta, G., Zini, N., Strusi, V., Dallatana, D., Toni, R. 2011. New approaches to prototype 3D vascular-like structures by additive layer manufacturing. In: P. Bártolo et al., eds., Innovative Developments in Virtual and Physical Prototyping. London: CRC Press, Taylor & Francis, 35-42.

[2] Bassoli, E., Denti, L., Gatto, A., Spaletta, G., Paderno, A., Zini, N., Parrilli, A., Giardino, R., Strusi, V., Dallatana, D., Mastrogiacomo, S., Zamparelli, A., Iafisco, M., Toni, R. 2012. A combined Additive Layer Manufacturing / Indirect Replication method to prototype 3D vascular-like structures of soft tissue and endocrine organs, Virtual and Physical Prototyping 7(1): 3-11.

[3] Fishman, E.K., Ney, D.R., Heath, D.G., Corl, F.M., Horton, K.M., Johnson, P.T. 2006. Volume rendering versus maximum intensity projection in CT angiography: what works best, when, and why. Radiographics 26(3):905-22.

[4] Liao, P.S., Chen, T.S., Chung, P.C. 2001. A Fast Algorithm for Multilevel Thresholding. J. of Information Science and Engineering 17:713-727.

[5] Major, R.H. 1909. Studies on the vascular system of the thyroid gland. Am. J. Anat. 9: 475–492.

[6] Mandelbrot, B.B. 1982. The fractal geometry of Nature. Freeman U.S.A.

[7] Otsu, N. 1979. A Threshold Selection Method from Gray-Level Histograms. IEEE Transaction on Systems, Man, and Cybernetics 9(1):62-66.

[8] Pal, N.R. & Pal, S.K. 1993. A review on image segmentation techniques. Pattern recognition 9:1277-1294

[9] Papadatos, D. 1981. Some anatomo-radiological observations concerning the changes in thyroid arteries which occur with senility. Anat. Anz. 150: 212-25.

[10] Parrilli, A., Zini, N., Spaletta, G., Bassoli, E., Gatto, A., Toni, R., Ceglia, L., Fini, M. 2013. Micro-CT of 3D vascular structures: clues to innovative scaffolds in organ engineering. In: Proc. of Micro-CT User Meeting, Hasselt (BE) 16-18 April 2013.

[11] Pavone, P., Luccichenti, G., Cademartiri, F. 2001. From maximum intensity projection to volume rendering. Semin Ultrasound CT MR 22(5):413-9

[12] Schreiner, W. and Buxbaum, P.F. 1993. Computer-optimization of vascular trees. IEEE Trans. Biomed. Eng. 40(5):482–491.

[13] Smith Jr., T.G., Lange, G.D., Marks, W.B. 1996. Fractal Methods and Results in Cellular Morphology. J. Neurosci. Methods 69:1123-1126

[14] Spaletta G. 2004. Reconstruction in space and visualization of a planar image: a mathematical and computational introduction. Acta Biomed 78 (1): 26-31.

[15] Toni, R., Della Casa, C., Spaletta, G., Marchetti, G., Mazzoni, P., Bodria, M., Ravera, S., Dallatana, D., Castorina, S., Riccioli, V., Castorina, E.G., Antoci, S., Campanile, E., Raise, G., Rossi, R., Ugolotti, G., Martorella, A., Roti, E., Sgallari, F., Pinchera, A., 2007. The bioartificial thyroid: a biotechnological perspective in endocrine organ engineering for transplantation replacement. Acta Biomed. 78 (1): 129–155.

[16] Toni, R., Della Casa, C., Bodria, M., Spaletta, G., Vella, R., Castorina, S., Gatto, A., Teti, G., Falconi, M., Rago, T., Vitti, P., Sgallari, F. 2008. A study on the relationship between intraglandular arterial distribution and thyroid lobe shape: Implications for biotechnology of a bioartificial thyroid. Annals of Anatomy 190 (5): 432-441.

[17] Toni, R., Tampieri, A., Zini, N., Strusi, V., Sandri, M., Dallatana, D., Spaletta, G., Bassoli, E., Gatto, A., Ferrari, A., Martin, I., 2011. Ex situ bioengineering of bioartificial endocrine glands: a new frontier in regenerative medicine of soft tissue organs. Annals of Anatomy 193, 381-394.

[18] Witten Jr, T.A., Sander, L.M., 1981. Diffusion Limited Aggregation, a Kinetic Critical Phenomenon. Physical Review Letters 47:1400-1403

[19] Wolfram, S. 2002. A New Kind of Science, Wolfram Media U.S.A.

[20] Zamir, M. 1982. Local geometry of arterial branching, Bulletin of Mathematical Biology 44(5): 597-607

[21] Zamir, M. 2001. Arterial Branching within the Confines of Fractal L-System Formalism. J. General Physiology 118:267–275.

[22] Gurpreet Singh Phull, Sanjeev Kumar, R.S. Walia, Conformal Cooling for Molds Produced by Additive Manufacturing: A Review, International Journal of Mechanical Engineering and Technology 9(1), 2018, pp. 1162–1172.